

---

# Papers

---

## Sea surface temperature distribution during upwelling along the Polish Baltic coast\*

OCEANOLOGIA, 47 (4), 2005.

pp. 415–432.

© 2005, by Institute of  
Oceanology PAS.

### KEYWORDS

Upwelling

Baltic

Sea surface temperature

AVHRR

ADAM KREŻEL

MICHAŁ OSTROWSKI

MARIA SZYMELFENIG

Institute of Oceanography,  
University of Gdańsk,  
al. Marszałka Piłsudskiego 46, PL–81–378 Gdynia, Poland;  
e-mail: oceak@univ.gda.pl

Received 21 February 2005, revised 26 September 2005, accepted 28 September 2005.

### Abstract

Among over 150 maps of sea surface temperature in the Polish Baltic coastal region derived from satellite data during the warm period of the year (April–October) in 2000–2002, 41 cases were noted where its distribution showed characteristic features indicating the occurrence of coastal upwelling. The fundamental parameters of range, probability of occurrence and temperature modification caused by water from deeper sea layers raised by an upwelling event and spreading across the surface were established for three regions (Hel, Łeba and Kołobrzeg). The Kołobrzeg upwelling region had the largest spatial range (up to 5000 km<sup>2</sup>). The region with the smallest spatial range (Hel, up to 1400 km<sup>2</sup>) had the largest surface temperature amplitude (to 14°C), the largest maximum temperature gradient (5°C km<sup>-1</sup>) and the largest average sea surface temperature decrease in the centre in relation to the background value.

---

\* This research was supported by the State Committee for Scientific Research, Poland (grant No 6 P04G 061 17). Editing assistance of the article was provided by BALTDER (EVK3-CT-2002-80005), funded by the European Commission under the 5th Framework Programme.

The complete text of the paper is available at <http://www.iopan.gda.pl/oceanologia/>

## 1. Introduction

Wind-driven upwelling of cold water is a process often observed off the coasts of oceans, marginal seas and large inland waters. Nowadays, sea surface temperature (SST) is relatively easy to determine by remote sensing. The results of investigations utilising satellite thermal imagery have shown this to be an effective tool for describing temporal and spatial SST variability patterns associated with upwelling fronts, cold filaments, mesoscale eddies, coastal morphology, and seasonal warming and cooling (Nykjær & Van Camp 1994, Fennel & Seifert 1995, Kahru et al. 1995, Kostianoy & Zatsepin 1996, Hernandez-Guerra & Nykjær 1997, Siegel et al. 1999, 2004, Askari 2001, Caldeira et al. 2002). Indeed, it was satellite imagery that brought to our attention the fact that coastal upwelling is a common occurrence in the Baltic Sea (Horstmann 1986, Bychkova & Viktorov 1987, Gidhagen 1987, Lass et al. 1994, 1996, Kowalewski & Ostrowski 2005).

SST is obtained by analysing the radiance recorded by radiometers sensitive to electromagnetic radiation in the c. 3.5–12.5  $\mu\text{m}$  range (thermal IR). This range includes so-called atmospheric windows, in which the influence of atmospheric components on sea surface-to-satellite signal transmission is minimal. As a result, relatively accurate measurement of the surface water temperature with a resolution of up to 0.1°C is possible. The absolute temperature is calculated by algorithms accounting for the atmospheric correlation as well as the skin temperature and the bulk temperature difference. The biggest drawback of this method, however, is that it can only be applied under clear skies. In the case of the Baltic Sea, therefore, the number of useful images is reduced to 10–50%, depending on season and weather conditions.

Coastal upwelling is one of the most significant factors affecting surface water temperatures and their spatial distribution along the Polish coast of the Baltic Sea (Bychkova & Viktorov 1987, Urbański 1995, Krężel 1997, Kowalewski 1998, Lehmann et al. 2002). In the warmer period of the year (from April to October), water raised to the surface from below the thermocline is clearly visible on satellite images because of its lower temperature. The intensity of upwelling and the significant temperature difference between surface and deep water often make it possible to trace the range and directions of the spreading cooler water on satellite images for as long as ten days, sometimes even longer. The shape and range of upwelling events appear to be linked with the strength and duration of the wind, and to some degree also with the bathymetry of the area in question. If these conditions do not change significantly in a given period

of time, then both the range and the shape of the plume will also remain unaltered.

Research carried out so far (Urbański 1995, Krężel 1997, Jankowski 2002, Kowalewski & Ostrowski 2005) has enabled certain regularities characterising upwelling along the Polish coast of the Baltic Sea to be defined: satellite images and the results of hydrodynamic modelling have identified at least four regions where the temperature of waters raised to the surface differs from the surroundings. Generally speaking, plumes of cooler water can be detected along the Polish coast when easterly winds generate an east-west surface coastal current. This was clearly illustrated by a simulation of temperature distributions and currents in this area (Jankowski 2002). Also, the distribution of these features suggests their division into a few regions, which can/should be considered separately. In the present study, areas of upwelling are identified as the Hel upwelling (1), Łeba upwelling (2) and Kołobrzeg upwelling regions (3). A fourth one, not analysed here, spreads along the Vistula Spit in the Gulf of Gdańsk. Fig. 1 shows the regions where typical surface water temperature distributions in the initial and developed stages of upwelling have been studied; it also shows the relevant bathymetry.

The aim of this study was to assess the quantitative characteristics and to specify surface temperature distribution regularities where upwelling occurs along the Polish coast of the Baltic Sea.

## 2. Material and method

AVHRR (Advanced Very High Resolution Radiometer) data from radiometers working on board the American TIROS-N/NOAA meteorological satellites (NOAA 12, 14, 15, 16 and 17) were used as the research material. The raw data were recorded by the receiving station of the Institute of Oceanography, University of Gdańsk (18°57'E, 54°40'N), then processed to sea surface temperature maps with a 1 km spatial resolution in the Laboratory of Remote Sensing and Spatial Analysis of the Department of Physical Oceanography. Operating continuously, the station receives signals from whichever of the three satellites is available at a given instant (e.g. NOAA 15, 16 or 17). If orbital parameters are taken into account, up to twelve images of the Baltic Sea can theoretically be stored daily. In practice, the number ranged from six to eleven. In order to determine the real surface temperature values, the MCSST linear split window algorithm (NOAA KLM User's Guide 2003) was applied to NOAA 12 and NOAA 14 data:

$$\text{MCSST} = a_1T_4 + a_2(T_4 - T_5) + a_3(T_4 - T_5)(\sec \theta - 1) + a_4, \quad (1)$$

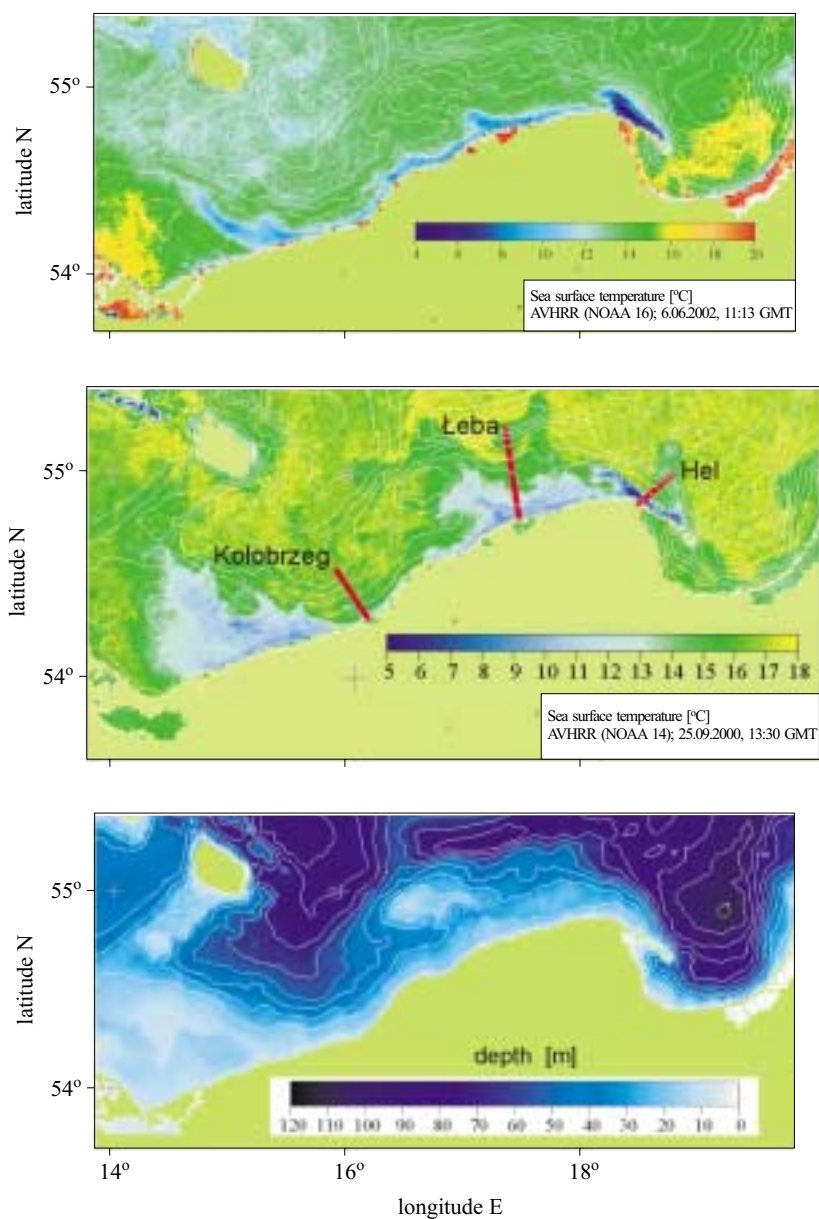


**Fig. 1.** The study area – example distributions of sea surface temperature in the southern Baltic during the initial (a) and developed (b) states of upwelling along the Polish coast; the bathymetry of the area (c). Red lines mark the profiles analysed in the article

and the NLSST non-linear split window (NOAA KLM User's Guide 2003) to NOAA 15, 16 and 17:

$$\text{NLSST} = b_1 T_4 + b_2 (T_4 - T_5) \text{MCSST} + b_3 (T_4 - T_5) (\sec \theta - 1) + b_4, \quad (2)$$

where  $T_4$  and  $T_5$  – respective brightness temperatures in AVHRR channels 4 and 5,  $\theta$  – zenith angle of the satellite,  $a_n$ ,  $b_n$  – empirical coefficients appropriate to the relevant satellite and time of day (night, day).

A set of equation coefficients (1) and (2) for the relevant satellites is presented in Table 1.

**Table 1.** Set of equation coefficients (1) & (2) for particular satellites and time of day (AVHRR... 2002)

| Satellite | Time  | Coefficients    |          |          |          |
|-----------|-------|-----------------|----------|----------|----------|
|           |       | MCSST algorithm |          |          |          |
|           |       | $a_1$           | $a_2$    | $a_3$    | $a_4$    |
| NOAA 12   | day   | 0.963563        | 2.579211 | 0.242598 | -263.006 |
| NOAA 12   | night | 0.967077        | 2.384376 | 0.480788 | -263.940 |
| NOAA 14   | day   | 1.017342        | 2.139588 | 0.779706 | -278.430 |
| NOAA 14   | night | 1.029088        | 2.275385 | 0.752567 | -282.240 |
| NOAA 15   | day   | 0.964243        | 2.712960 | 0.387491 | -262.443 |
| NOAA 15   | night | 0.976789        | 2.770720 | 0.435832 | -266.290 |
| NOAA 16   | day   | 0.999314        | 2.301950 | 0.628976 | -273.768 |
| NOAA 16   | night | 0.995103        | 2.536570 | 0.753281 | -273.146 |
| NOAA 17   | day   | 0.992818        | 2.499160 | 0.915103 | -271.206 |
| NOAA 17   | night | 1.010150        | 2.581500 | 1.000540 | -276.590 |
|           |       | NLSST algorithm |          |          |          |
|           |       | $b_1$           | $b_2$    | $b_3$    | $b_4$    |
| NOAA 12   | day   | 0.876992        | 0.083132 | 0.349877 | -236.667 |
| NOAA 12   | night | 0.888706        | 0.081646 | 0.576136 | -240.229 |
| NOAA 14   | day   | 0.939813        | 0.076060 | 0.801458 | -255.165 |
| NOAA 14   | night | 0.933109        | 0.078095 | 0.738128 | -253.428 |
| NOAA 15   | day   | 0.913116        | 0.090576 | 0.476940 | -246.887 |
| NOAA 15   | night | 0.922560        | 0.093611 | 0.548055 | -249.819 |
| NOAA 16   | day   | 0.914471        | 0.077612 | 0.668532 | -248.116 |
| NOAA 16   | night | 0.898887        | 0.083933 | 0.755283 | -244.006 |
| NOAA 17   | day   | 0.936047        | 0.083867 | 0.920848 | -253.951 |
| NOAA 17   | night | 0.938875        | 0.086427 | 0.979108 | -255.023 |

Since waters elevated by upwelling to the sea surface can be identified on the basis of temperature, only images registered in the warmer period of the year (April–October) were analysed; they were separated from each other in time by at least 6 hours, and the cloud cover did not exceed 20%. At this time of year, the temperature of this water is much lower than that

of the surface water and is thus fairly easy to detect. A total of 150 images covering the Polish coast of the southern Baltic and fulfilling the above criteria were examined. Upwelling was identified on 41 of them, and it is these images that were subjected to analysis.

The range of spreading cool water was specified by analysis of the horizontal temperature gradient on the offshore transect (the red lines in Fig. 1) through its range in each of the three regions defined on the basis of recent research. As a result, a threshold temperature dividing upwelled from non-upwelled water was established. Identical on all the maps of a given region, the transects were made to cross the centre of the upwelling area, i.e. where minimum temperatures occurred the most frequently; they also included some of the background region. The threshold value was taken to be the temperature in an area of a horizontal gradient falling very steeply towards the open sea (practically to 0). Fig. 2 gives an example of this. In this particular case the threshold temperature was 16°C, recorded 5 km from the start of the profile. In order to compare temperature changes along the profiles, values obtained in different seasons were standardised according to the following relation:

$$T_s = \frac{T - T_t}{T_t}, \quad (3)$$

where  $T_s$  – standardised temperature,  $T$  – sea surface temperature in a given area of the cross-section,  $T_t$  – background temperature of the region surrounding the upwelling water plume.

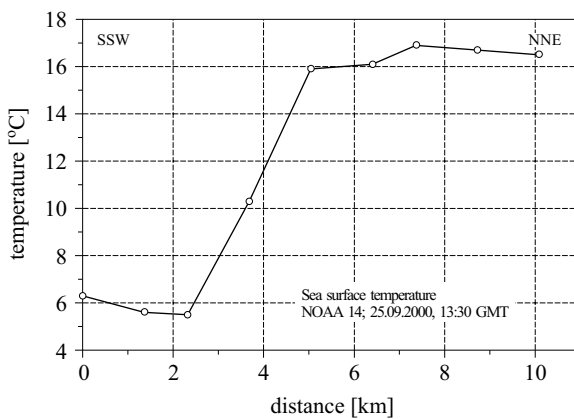


**Fig. 2.** Sea surface temperature in the cross-section of the Hel upwelling region

The spatial extent of upwelled water was obtained by overlapping all the analysed maps of the range, and making the following assumption: if upwelled water was always recorded in a given place, then the probability

of it occurring there again is equal to 100%; if it was recorded only in half of the cases, this probability is 50%, and so on. Bearing in mind that the method of range specification is not one hundred percent accurate, the scale was limited to the range 30–100%.

The area of sea around the upwelling centre (the lowest temperature in the region) as far as the threshold temperature isotherm was assumed to be under the influence of the event. It is further referred to as the region of ‘upwelling water’.

### 3. Results and discussion

The surface temperature distributions in the southern Baltic Sea at different times of the day in the period 4–15 May 2000 are presented in Fig. 3. On each image, regions where the water temperature is significantly lower than that of the surroundings are delineated in red. Comparison of their shapes and ranges with the results published in other studies (Bychkova & Viktorov 1987, Urbański 1995, Krężel 1997) shows clearly that they are identical to those identified earlier as a result of a coastal upwelling occurrence. This is also justified by the confirmed hypothesis that the duration of an upwelling event is at least a few days.

The influence of upwelling on the surface water temperature in three regions was traced, for example, in the cross-sectional profiles described earlier and presented in Fig. 1b.

#### 3.1. Hel upwelling region

Previous studies of coastal upwelling in the Baltic Sea have indicated its significance in the area around the Hel Peninsula (Urbański 1995, Krężel 1997). This significance is based on the higher frequency of such events there than elsewhere, their powerful dynamics (a brief generation period followed by rapid fading) and the wide range of wind directions bringing them about. Also, it is here that the horizontal temperature distribution gradients are steepest: satellite images with a spatial resolution of 1 km show that these gradients can be as steep as  $5.2^{\circ}\text{C km}^{-1}$  (Fig. 2). The temperature difference between upwelled deep water and surface water depends primarily on the actual temperature of the surface water and the intensity of upwelling. The largest such difference –  $12.4^{\circ}\text{C}$  – was recorded in this region on 5.09.2000. Generally, these differences are greatest in summer and early autumn. The minimum temperature of the deep water lifted up to the surface is usually  $< 10^{\circ}\text{C}$  (Table 2). The extent and other characteristic features of the surface temperature in the Hel Peninsula region are well illustrated in Fig. 4a.

This presents the basic temperature statistics indicated on the transect, marked on Fig. 1b as ‘Hel’. An area covered by water of a temperature lower

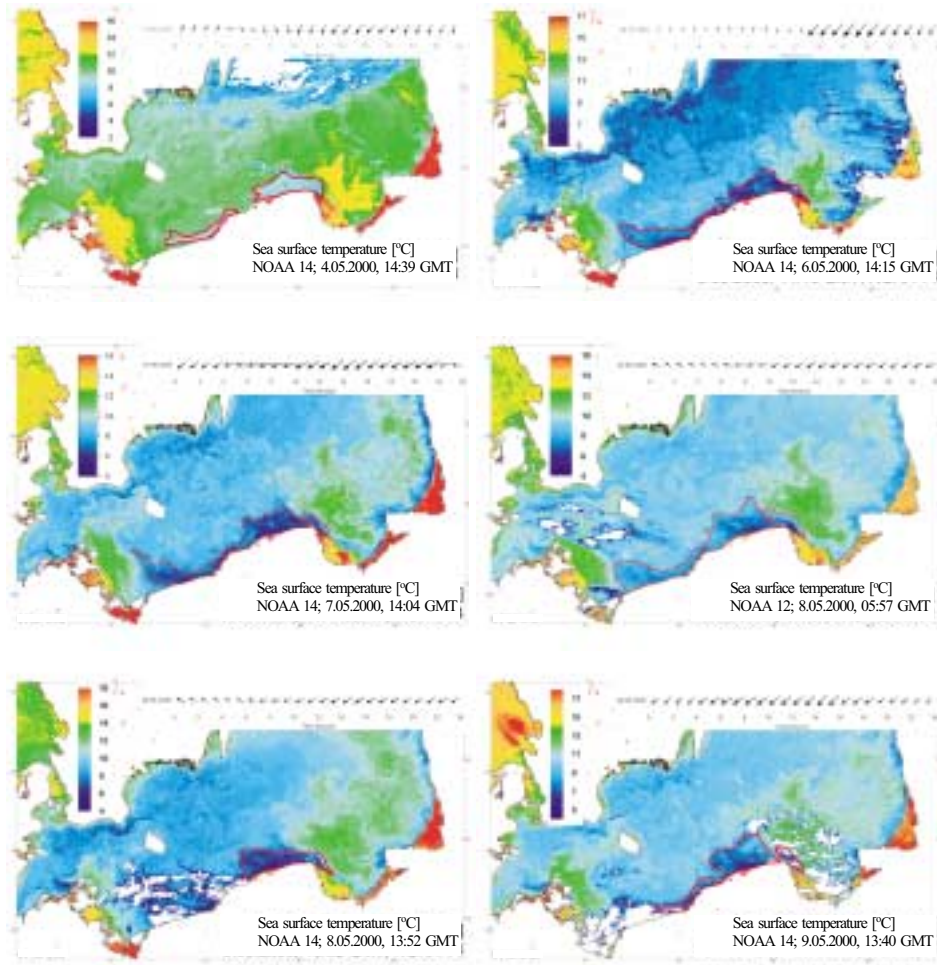


**Fig. 3.** Sea surface temperature distribution in the southern Baltic on 6–16 May 2000. Marked areas indicate lower temperatures, which may be related to coastal upwelling. The arrows in the upper part indicate the wind history about 16 km off the coast at  $18^{\circ}31.094'E$  and  $54^{\circ}56.157'N$  on the day in question

than that of the surroundings displays the following features: (i) the width of the area is about 18 km (in the cross-section in Fig. 4), (ii) its location c. 1.5–5 km along the transect from its origin on the coast, and (iii) the extent of the drop in temperature, which at the upwelling centre is from c. 30 to 70% (average 50%) of the temperature of the surroundings.

The spatial range of the water in the Hel upwelling region is presented in Fig. 4b. This shows the probability of cooler water from deeper sea layers spreading on to the surface. The region where the probability of water rising

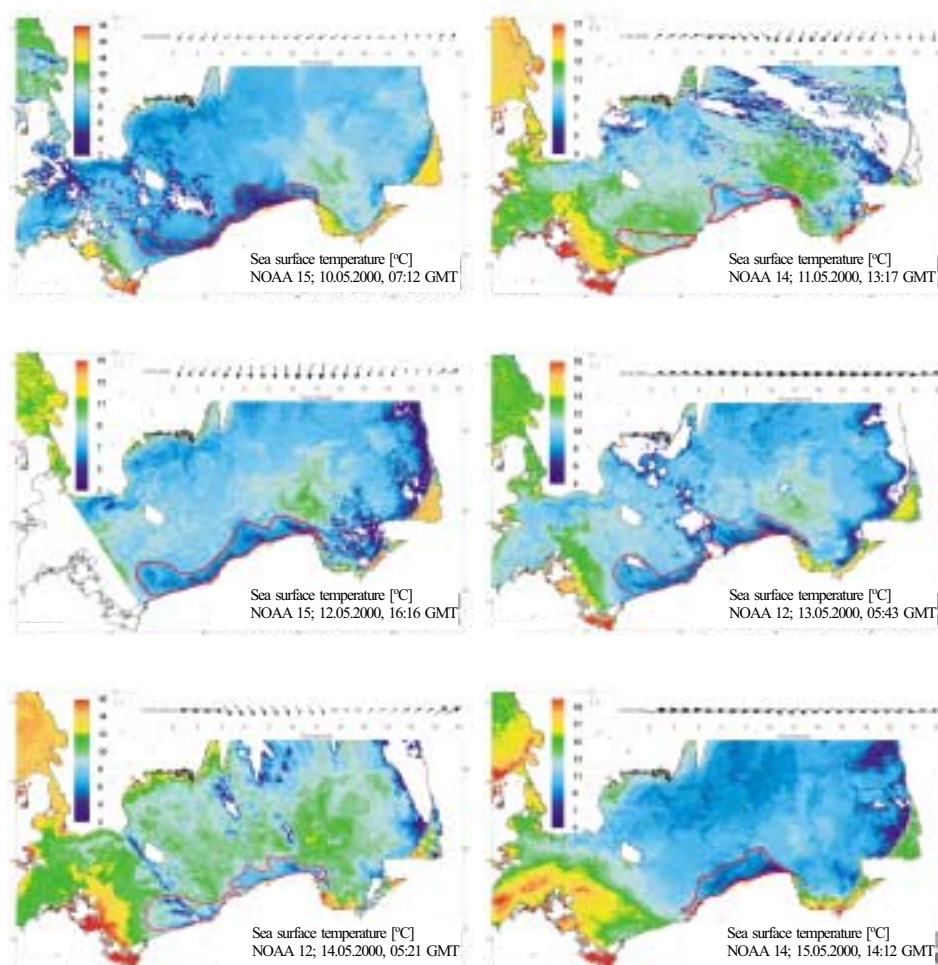


**Fig. 3.** (*continued*)

from deeper layers is  $> 50\%$  is  $250 \text{ km}^2$  in area. Its centre lies 4.5 km from the coast, at the point where the following coordinates cut:  $54^\circ 50' \text{N}$ ,  $18^\circ 28' \text{E}$ .

### 3.2. Łeba upwelling region

In its fully developed state, the Łeba upwelling region covers an area almost three times larger than that off the Hel peninsula. The maximum temperature difference recorded on any specific transect was  $12.3^\circ \text{C}$  (Table 3), which means that it was only  $0.1^\circ \text{C}$  lower than in the case of the Hel region. In contrast, however, the temperature differentiation is significantly lower. The mean variance is almost half as large (c.  $4.5^\circ \text{C}$ ). On the cross-section marked 'Łeba' (Figs 1b and 5a) the area of upwelling water

**Table 2.** Statistical characteristics of temperatures [°C] on the Hel cross-section

| Date       | Mean  | Min   | Max  | Range | Variance | SD    |      |
|------------|-------|-------|------|-------|----------|-------|------|
| 01.05.2000 | 15:03 | 7.46  | 2.9  | 11.7  | 8.8      | 11.32 | 3.37 |
| 02.05.2000 | 16:40 | 6.04  | 2.4  | 9.4   | 7.0      | 7.42  | 2.72 |
| 03.05.2000 | 13:10 | 7.68  | 3.2  | 12.0  | 8.8      | 8.30  | 2.88 |
| 04.05.2000 | 14:39 | 7.89  | 4.9  | 11.1  | 6.2      | 5.03  | 2.24 |
| 06.05.2000 | 14:15 | 7.68  | 3.2  | 12.0  | 8.8      | 8.30  | 2.88 |
| 07.05.2000 | 04:39 | 7.20  | 2.7  | 10.8  | 8.1      | 7.86  | 2.80 |
| 07.05.2000 | 14:04 | 9.09  | 6.0  | 11.4  | 5.4      | 3.38  | 1.84 |
| 08.05.2000 | 03:59 | 7.06  | 3.2  | 10.5  | 7.3      | 8.00  | 2.83 |
| 08.05.2000 | 04:16 | 7.01  | 3.0  | 10.8  | 7.8      | 8.40  | 2.90 |
| 08.05.2000 | 07:56 | 6.64  | 3.1  | 9.7   | 6.6      | 5.44  | 2.33 |
| 08.05.2000 | 15:47 | 9.49  | 5.4  | 12.1  | 6.7      | 6.17  | 2.48 |
| 09.05.2000 | 17:25 | 7.19  | 2.7  | 10.1  | 7.4      | 5.50  | 2.35 |
| 17.09.2000 | 05:55 | 13.24 | 6.5  | 17.3  | 10.8     | 19.68 | 4.44 |
| 17.09.2000 | 15:43 | 14.57 | 6.5  | 17.7  | 11.2     | 16.43 | 4.05 |
| 18.09.2000 | 13:12 | 14.02 | 5.3  | 17.3  | 12.0     | 16.94 | 4.12 |
| 23.09.2000 | 13:53 | 13.60 | 7.0  | 16.2  | 9.2      | 7.82  | 2.80 |
| 25.09.2000 | 04:32 | 12.01 | 3.5  | 15.9  | 12.4     | 18.61 | 4.31 |
| 25.09.2000 | 13:30 | 14.66 | 7.4  | 16.5  | 9.1      | 4.93  | 2.22 |
| 26.09.2000 | 03:25 | 13.13 | 7.3  | 15.2  | 7.9      | 6.87  | 2.62 |
| 29.09.2000 | 14:24 | 11.81 | 6.4  | 17.4  | 11.0     | 16.11 | 4.01 |
| 30.09.2000 | 04:19 | 13.02 | 5.2  | 15.9  | 10.7     | 14.55 | 3.81 |
| 30.09.2000 | 14:12 | 12.13 | 5.8  | 15.6  | 9.8      | 13.97 | 3.74 |
| 15.10.2000 | 14:37 | 8.88  | 7.0  | 12.7  | 5.7      | 2.52  | 1.59 |
| 16.10.2000 | 04:52 | 5.82  | 3.6  | 8.0   | 4.4      | 1.81  | 1.35 |
| 16.10.2000 | 14:25 | 8.99  | 7.1  | 11.3  | 4.2      | 3.04  | 1.74 |
| 16.10.2000 | 14:41 | 8.68  | 6.7  | 11.6  | 4.9      | 3.08  | 1.76 |
| 19.10.2000 | 13:50 | 10.34 | 7.5  | 13.5  | 6.0      | 5.21  | 2.28 |
| 08.07.2001 | 04:37 | 20.70 | 19.1 | 22.9  | 3.8      | 1.63  | 1.28 |
| 11.05.2002 | 06:29 | 9.28  | 5.8  | 14.0  | 8.2      | 5.86  | 2.42 |
| 03.09.2002 | 10:05 | 7.57  | 2.9  | 14.5  | 11.6     | 12.94 | 3.60 |

Min – minimum value, Max – maximum value, SD – standard deviation.

is centred around 6 km from the shore and is over 25 km wide. On average, the water temperature in the centre of an upwelling region is 20 to 50% lower than the background value. The region where upwelled water spreading on to the surface can be detected with 30% probability is  $> 3000 \text{ km}^2$  in area and extends roughly 40 km from the coast. The centre of this upwelling

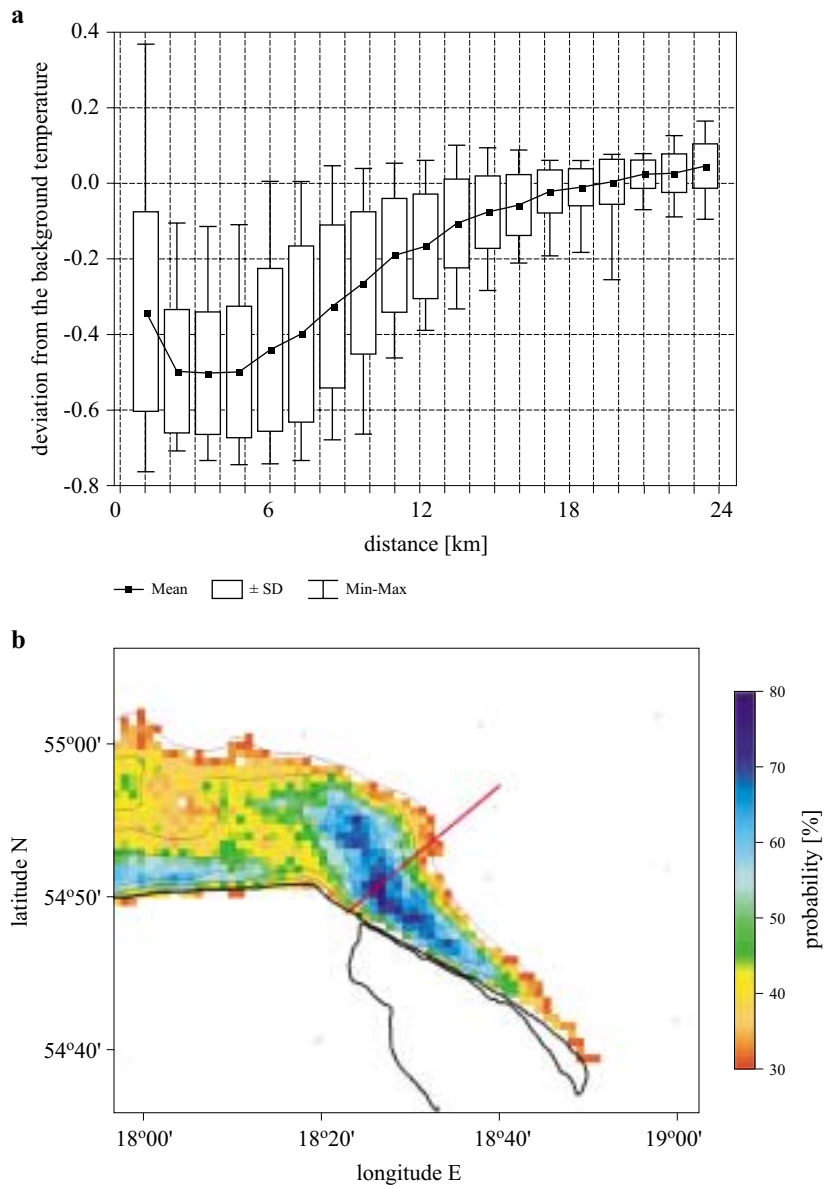


**Fig. 4.** Sea surface temperature (standardised) distribution on the Hel cross-section (a) and the probability of upwelled water appearing on the sea surface (b) during an upwelling event

stretches for some 80 km along the shore in the form of a narrow strip 4–8 km wide. Its surface area is estimated to be 800 km<sup>2</sup> (Fig. 5b). Within its boundaries there are areas where the probability of an upwelling event is as high as 75%.

**Table 3.** Statistical characteristics of temperatures [°C] on the Łeba cross-section

| Date       | Mean  | Min   | Max  | Range | Variance | SD    |      |
|------------|-------|-------|------|-------|----------|-------|------|
| 02.05.2000 | 15:03 | 6.91  | 3.6  | 13.4  | 9.8      | 6.44  | 2.54 |
| 02.05.2000 | 16:40 | 4.55  | 2.2  | 7.6   | 5.4      | 2.60  | 1.61 |
| 03.05.2000 | 13:10 | 7.41  | 5.1  | 10.1  | 5.0      | 2.72  | 1.65 |
| 04.05.2000 | 14:39 | 7.85  | 1.7  | 14.0  | 12.3     | 5.22  | 2.29 |
| 06.05.2000 | 14:15 | 8.93  | 5.4  | 13.2  | 7.8      | 3.19  | 1.79 |
| 07.05.2000 | 04:39 | 6.81  | 3.8  | 9.8   | 6.0      | 4.33  | 2.08 |
| 08.05.2000 | 15:47 | 8.35  | 4.4  | 12.0  | 7.6      | 6.85  | 2.62 |
| 09.05.2000 | 17:25 | 6.58  | 3.4  | 9.8   | 6.4      | 3.74  | 1.93 |
| 15.05.2000 | 07:02 | 7.68  | 5.2  | 10.1  | 4.9      | 2.80  | 1.67 |
| 17.09.2000 | 13:23 | 14.40 | 12.0 | 16.9  | 4.9      | 2.23  | 1.49 |
| 18.09.2000 | 13:12 | 13.10 | 9.3  | 17.0  | 7.7      | 6.99  | 2.64 |
| 22.09.2000 | 15:29 | 12.15 | 8.6  | 16.7  | 8.1      | 9.23  | 3.04 |
| 23.09.2000 | 13:53 | 12.93 | 8.2  | 17.3  | 9.1      | 11.17 | 3.34 |
| 25.09.2000 | 13:30 | 13.87 | 9.1  | 17.3  | 8.2      | 8.27  | 2.87 |
| 29.09.2000 | 14:24 | 13.58 | 9.7  | 17.2  | 7.5      | 6.14  | 2.48 |
| 30.09.2000 | 14:12 | 11.43 | 7.1  | 15.9  | 8.8      | 8.20  | 2.86 |
| 03.10.2000 | 13:37 | 12.70 | 9.9  | 15.5  | 5.6      | 2.88  | 1.70 |
| 15.10.2000 | 14:37 | 9.99  | 7.8  | 12.6  | 4.8      | 1.88  | 1.37 |
| 16.10.2000 | 14:25 | 9.48  | 6.7  | 14.4  | 7.7      | 8.18  | 2.86 |
| 19.10.2000 | 13:50 | 9.59  | 7.2  | 14.3  | 7.1      | 3.46  | 1.86 |
| 08.07.2001 | 04:37 | 20.21 | 16.1 | 22.1  | 6.0      | 2.58  | 1.61 |
| 11.05.2002 | 06:29 | 8.58  | 7.2  | 10.1  | 2.9      | 0.97  | 0.98 |
| 06.06.2002 | 11:13 | 13.39 | 8.4  | 14.9  | 6.5      | 3.00  | 1.73 |
| 19.08.2002 | 15:31 | 20.74 | 16.9 | 23.3  | 6.4      | 2.73  | 1.65 |
| 20.08.2002 | 02:41 | 17.93 | 13.7 | 20.4  | 6.7      | 2.97  | 1.72 |
| 03.09.2002 | 10:05 | 20.11 | 17.7 | 21.1  | 3.4      | 1.09  | 1.04 |

Min – minimum value, Max – maximum value, SD – standard deviation.

### 3.3. Kołobrzeg upwelling region

The surface area of upwelled water spreading on to the sea surface is the largest in this region (Fig. 6). The reason for this most probably lies in its bathymetry. Water upwelled to the surface is usually directed north-westwards by the edge of the Ławica Odrzana (Odra Bank), which covers an area of up to 5000 km<sup>2</sup>. However, over half of this area lies in a region where the probability of upwelling is < 30%. The ‘power’ of upwelling events here is similar to that in the Łeba region (Table 4). However, the temperature at the centre of the upwelling in relation to the background falls from 10 to 45% (av. 25%), i.e. it is the lowest of the three regions analysed. The cross-section where the temperature is almost always lower than the background

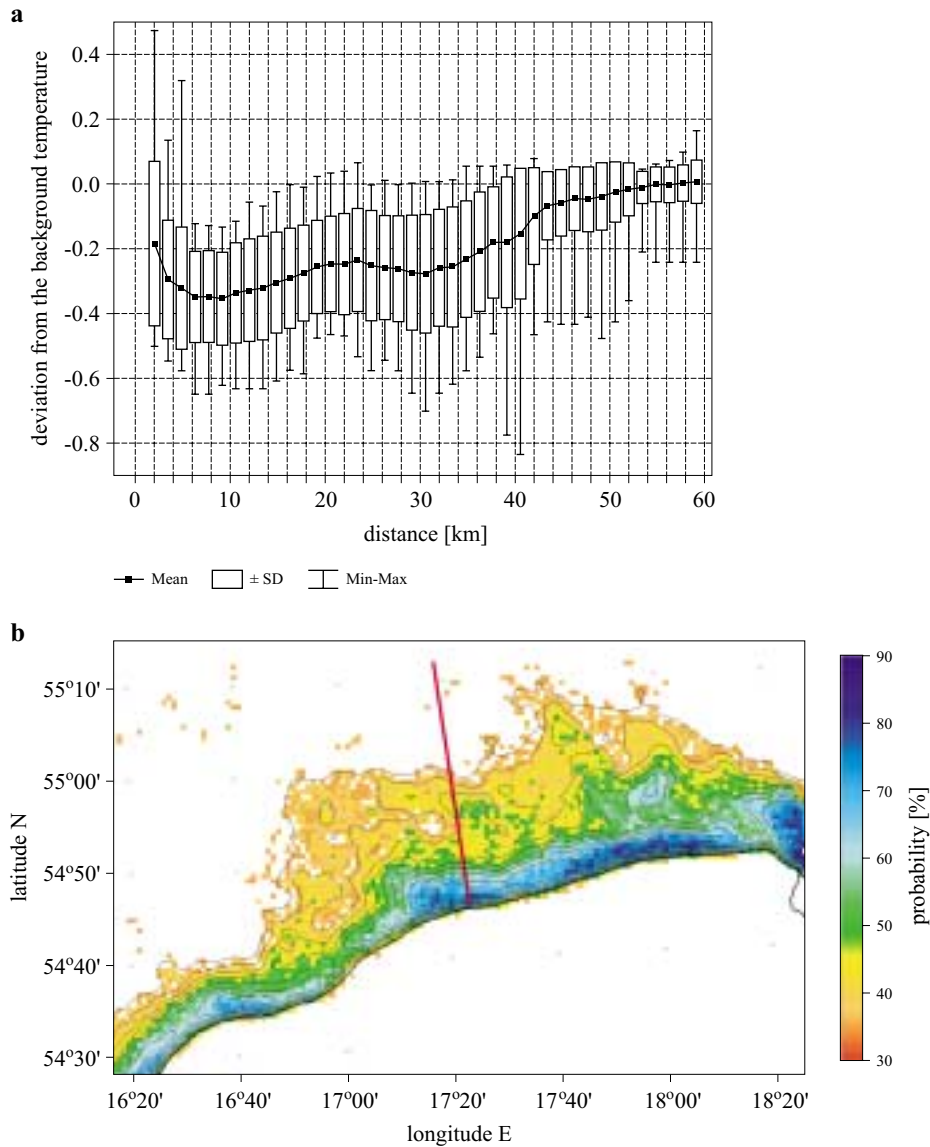


**Fig. 5.** Sea surface temperature (standardised) distribution on the Łeba cross-section (a) and the probability of upwelled water appearing on the sea surface (b) during an upwelling event

value should upwelling occur is c. 16 km wide. The region with the lowest temperatures extends along the coast for 100 km and is 6 to 10 km from the upwelling centre, where in around 75% of upwelling events, upwelling water can be detected at 16°05'E, 54°17'N, that is some 35 km to the east of Kołobrzeg, and only 1–1.5 km offshore.

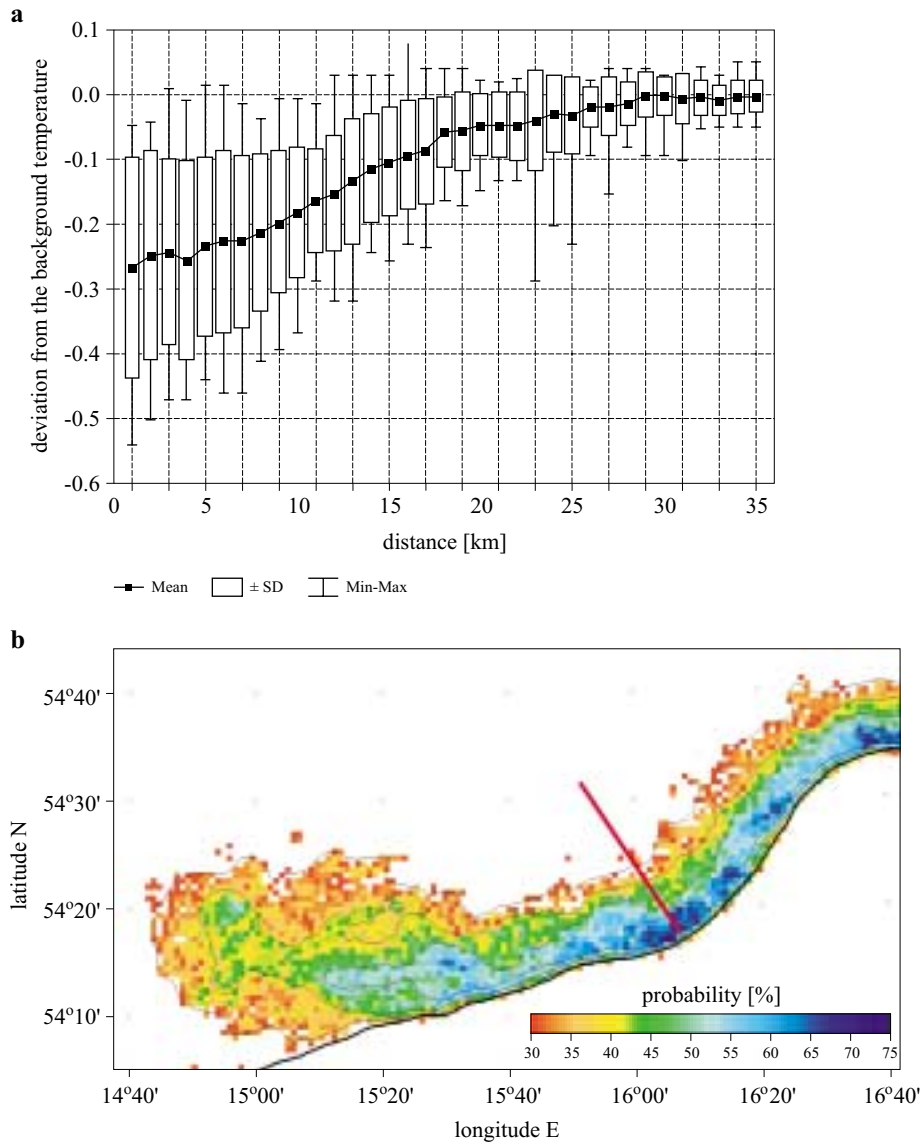


**Fig. 6.** Sea surface temperature (standardised) distribution on the Kołobrzeg cross-section (a) and the probability of upwelled water appearing on the sea surface (b) during an upwelling event

Analysis of surface water temperatures on the basis of the criteria set out earlier enabled the maximum range of upwelling on the sea surface to be determined. The surface area covered by water cooler than the surroundings decreased in the following order: Kołobrzeg upwelling region (c. 5000 km<sup>2</sup>), Łeba (up to c. 3500 km<sup>2</sup>), Hel (c. 1400 km<sup>2</sup>). These three upwelling regions

**Table 4.** Statistical characteristics of temperatures [°C] on the Kołobrzeg cross-section

| Date             | Mean  | Min  | Max  | Range | Variance | SD   |
|------------------|-------|------|------|-------|----------|------|
| 02.05.2000 15:03 | 8.05  | 6.3  | 9.0  | 2.7   | 0.75     | 0.87 |
| 04.05.2000 14:39 | 19.14 | 18.2 | 20.8 | 2.6   | 0.74     | 0.86 |
| 06.05.2000 14:15 | 8.29  | 7.1  | 9.7  | 2.6   | 0.63     | 0.79 |
| 07.05.2000 14:04 | 7.26  | 5.3  | 8.4  | 3.1   | 0.94     | 0.97 |
| 08.05.2000 03:59 | 6.86  | 4.7  | 8.1  | 3.4   | 0.90     | 0.95 |
| 15.05.2000 07:02 | 9.07  | 8.2  | 9.7  | 1.5   | 0.20     | 0.45 |
| 18.09.2000 13:12 | 14.52 | 11.6 | 16.8 | 5.2   | 3.29     | 1.81 |
| 21.09.2000 04:24 | 13.22 | 7.2  | 16.1 | 8.9   | 9.45     | 3.07 |
| 22.09.2000 15:29 | 12.36 | 8.1  | 15.2 | 7.1   | 5.92     | 2.43 |
| 23.09.2000 13:53 | 12.91 | 8.3  | 15.9 | 7.6   | 6.48     | 2.55 |
| 25.09.2000 13:30 | 14.44 | 8.9  | 17.2 | 8.3   | 7.98     | 2.83 |
| 29.09.2000 14:24 | 14.09 | 10.2 | 17.2 | 7     | 4.32     | 2.08 |
| 30.09.2000 14:12 | 11.80 | 7.7  | 14.8 | 7.1   | 5.97     | 2.44 |
| 16.10.2000 04:52 | 8.74  | 7.2  | 10.4 | 3.2   | 0.74     | 0.86 |
| 06.06.2002 11:13 | 13.32 | 9.0  | 14.9 | 5.9   | 1.42     | 1.19 |
| 19.08.2002 12:45 | 19.22 | 18.5 | 20.2 | 1.7   | 0.25     | 0.50 |
| 20.08.2002 12:34 | 20.54 | 19.3 | 21.3 | 2     | 0.32     | 0.57 |
| 03.09.2002 10:05 | 19.14 | 18.2 | 20.8 | 2.6   | 0.74     | 0.86 |

Min – minimum value, Max – maximum value, SD – standard deviation.

approximately cover the area shown in Fig. 1. Since the method of specifying the criteria defining the border between upwelling and surface water is subjectively biased, all the values given here to delineate the range of an upwelling event should be treated as estimates for defining the scale of the occurrence.

As a result of our analysis several known regularities related to this phenomenon were confirmed and the parameters describing principally its spatial range and intensity were specified more accurately.

Analysis of the shape and size of the features of cooler water as the outcome of an upwelling event confirmed that they are due to bathymetry (cf. Figs 1b and 1c), the characteristics of surface flows and the intensity of the event. These are also the factors influencing the division of upwelling into these three distinctive regions. The borders between them are the result of flow characteristics, which have also been well observed in modelled simulations (Jankowski 2002). The direction of spreading indicates that upwelling is generated in line with Ekman's classic theory. According to this, upwelling in the Polish coastal region comes about as a result of a coastal current induced by easterly winds. A certain departure from this rule, i.e.

the occurrence of upwelling when winds blow from other directions, has been observed only in the Hel upwelling region (J. A. Urbański, personal communication).

The spatial ranges of water raised by upwelling and spreading over the surface in the three regions are presented on maps 4b, 5b and 6b. It should be noted that the shape in the Hel region is very similar to the results of the principal component analysis (PCA) of temperature distribution in this area presented by J. A. Urbański (pers. comm.). The image in Fig. 4b is almost exactly the same as the image of the first component.

**Table 5.** Characteristics of the spatial distribution of upwelling water along the Polish coastline

| Feature                                                                                     | Hel   | Łeba  | Kołobrzeg |
|---------------------------------------------------------------------------------------------|-------|-------|-----------|
| Maximum area of spill [km <sup>2</sup> ]                                                    | 1400  | 3500  | 5000      |
| Area of occurrence with a probability of at least [km <sup>2</sup> ]                        | 30%   | 700   | 2800      |
|                                                                                             | 75%   | 10    | 200       |
| Maximum difference of temperature [°C]                                                      | 14    | 12.3  | 8.9       |
| Maximum gradient of temperature [°C km <sup>-1</sup> ]                                      | 5.3   | 5     | 3.5       |
| Mean decrease of standardised temperature in the centre in comparison to the background [%] | 30–70 | 20–50 | 10–45     |

Some characteristic features of upwelling water in particular regions are presented in Table 5. The potential maximum area of all upwellings off the Polish coast is almost 10 000 km<sup>2</sup>, which makes up about 30% of the Polish economic zone. Upwelling is the most dynamic off the shores of the Hel Peninsula, since this is where the temperature differences and horizontal gradients are the greatest. The area of water elevation to the surface is also the most concentrated here. In the other regions, the dynamics of upwelling are significantly less – this is expressed by the lower temperature differences and gentler gradients. However, the horizontal range is up to four times more extensive. It is therefore assumed that the basic reason for this diversification is depth of the sea and the configuration of the sea bed.

## References

- Askari F., 2001, *Multi-sensor remote sensing of eddy-induced upwelling in the southern coastal region of Sicily*, Int. J. Remote Sens., 22 (15), 2899–2910.
- AVHRR Sea Surface Temperature Products, 2002, [[http://coastwatch.noaa.gov/poes\\_sst\\_algorithms.html](http://coastwatch.noaa.gov/poes_sst_algorithms.html)].

- Bychkova I. A., Viktorov S. V., 1987, *Use of satellite data for identification and classification of upwelling in the Baltic Sea*, *Oceanology*, 27 (2), 158–162.
- Caldeira R. M. A., Groom S., Miller P., Pilgrim D., Nezlin N. P., 2002, *Sea surface signatures of the island mass effect phenomena around Madeira Island, Northeast Atlantic*, *Remote Sens. Environ.*, 80 (2), 336–360.
- Fennel W., Seifert T., 1995, *Kelvin wave controlled upwelling in the western Baltic*, *J. Marine Syst.*, 6 (4), 289–300.
- Gidhagen L., 1987, *Coastal upwelling in the Baltic – satellite and in situ measurements of sea surface temperatures indicating coastal upwelling*, *Estuar. Coast. Shelf Sci.*, 24 (4), 449–462.
- Hernandez-Guerra A., Nykjær L., 1997, *Sea surface temperature variability off north-west Africa: 1981–1989*, *Int. J. Remote Sens.*, 18 (12), 2539–2558.
- Horstmann U., 1986, *Remote sensing of sea surface temperature and water colour anomalies in the southern Baltic Sea*, *Bull. Sea Fish. Inst.*, 17 (5)–(6), 11–17.
- Jankowski A., 2002, *Variability of coastal water hydrodynamics in the southern Baltic – hindcast modelling of an upwelling event along the Polish coast*, *Oceanologia*, 44 (4), 395–418.
- Kahru M., Håkansson B., Rud O., 1995, *Distributions of the sea-surface temperature fronts in the Baltic Sea as derived from satellite imagery*, *Cont. Shelf Res.*, 15 (6), 663–679.
- Kostianoy A. G., Zatsepin A. G., 1996, *The West African coastal upwelling filaments and cross-frontal water exchange conditioned by them*, *J. Marine Syst.*, 7 (2)–(4), 349–359.
- Kowalewski M., 1998, *Coastal upwellings in a shallow stratified sea on the example of the Baltic Sea*, Ph. D. thesis, Institute of Oceanography, Univ. Gd., Gdynia, 83 pp., (in Polish).
- Kowalewski M., Ostrowski M., 2005, *Coastal up- and downwelling in the southern Baltic*, *Oceanologia*, 47 (4), (435–475).
- Kreżel A., 1997, *Recognition of mesoscale hydrophysical anomalies in a shallow sea using broadband satellite remote sensing methods*, Diss. and monogr., Univ. Gd., Gdynia, 173 pp., (in Polish).
- Lass H.-U., Schmidt T., Seifert T., 1994, *On the dynamics of upwelling observed at the Darss Sill*, *Proc. 19th Conf. Baltic Oceanogr.*, Sopot, 247–260.
- Lass H.-U., Schmidt T., Seifert T., 1996, *Hiddensee upwelling field measurements and modelling results*, *ICES Coop. Res. Rep. No 257*, 204–208.
- Lehmann A., Krauss W., Hinrichsen H.-H., 2002, *Effects of remote and local forcing on circulation and upwelling in the Baltic Sea*, *Tellus*, 54 (A), 299–316.
- NOAA KLM User's Guide, Appendix G.3, 2003, [<http://www2.ncdc.noaa.gov/docs/klm/html/g/app-g3.htm>].
- Nykjær L., Van Camp L., 1994, *Seasonal and interannual variability of coastal upwelling along northwest Africa and Portugal from 1981–1991*, *J. Geophys. Res.*, 99 (C7), 14197–14207.

- Siegel H., Gerth M., Tiesel R., Tschersich G., 1999, *Seasonal and interannual variations in satellite derived sea surface temperature of the Baltic Sea in the 1990's*, Dt. Hydrogr. Z., 51 (4), 407–422.
- Siegel H., Seifert T., Gerth M., Ohde T., Reissmann J., Schernewski G., 2004, *Dynamical processes along the German Baltic Sea coast systematised to support coastal monitoring*, Coastline Rep. No 2, 219–226.
- Urbański J. A., 1995, *Upwellings of the Polish coast of the Baltic Sea*, Prz. Geofiz., 40 (2), 141–153, (in Polish).